NATIONAL ADVISORY COMMITTEE FOR AERONAUTICS

TECHNICAL NOTE 4302

ANALYTICAL AND EXPERIMENTAL INVESTIGATION OF AERODYNAMIC FORCES AND MOMENTS ON LOW-ASPECT-RATIO WINGS UNDERGOING FLAPPING OSCILLATIONS

By Donald S. Woolston, Sherman A. Clevenson, and Sumner A. Leadbetter

Langley Aeronautical Laboratory
Langley Field, Va.

NACA

Washington
August 1958

NATIONAL ADVISORY COMMITTEE FOR AERONAUTI

TECHNICAL NOTE 4302

ANALYTICAL AND EXPERIMENTAL INVESTIGATION OF AERODYNAMIC FORCES AND MOMENTS ON LOW-ASPECT-RATIO WINGS UNDERGOING FLAPPING OSCILLATIONS

By Donald S. Woolston, Sherman A. Clevenson, and Sumner A. Leadbetter

SUMMARY

Aerodynamic forces and moments associated with flapping oscillations of finite wings at low speeds are considered. A comparison of theoretical and experimental results is made for a rectangular wing of aspect ratio 2. Calculated results are also given for three tapered wings of aspect ratio 3 with varying amounts of sweepback. The calculations are based on a numerical solution of the integral equation of subsonic lifting-surface theory. The experimental techniques employed are essentially those used in previous measurements associated with pitching oscillations. Theory and experiment are generally in good agreement with regard to magnitude of the forces and moments, but differ with regard to phase angle.

INTRODUCTION

Until recently the treatment of the aerodynamic portion of the flutter problem has been based primarily on the two-dimensional theory of oscillating wings. Generalized aerodynamic coefficients required for flutter analysis have normally been obtained by various strip-analysis methods in which two-dimensional section coefficients associated with rigid mode displacements, such as translation and pitch, are used together with actual spanwise variations in displacement. With the increasing need for more accurately predicted flutter boundaries, however, attempts have been made to obtain more accurately the aerodynamic components of the flutter problem. Considerable effort has been directed toward the experimental measurement of oscillatory aerodynamic forces and moments. In reference 1, for example, measured forces and moments are presented for the case of pitching oscillations for one of the configurations dealt with in the present investigation.

Efforts have also been made in the direction of increasing accuracy in the theoretical determination of oscillatory aerodynamics. With the aid of advances in high-speed computing equipment, procedures have been developed for obtaining the aerodynamic forces associated with the particular plan form of interest and with its specific modes of oscillation. One such procedure, a numerical solution of the integral equation of subsonic lifting-surface theory, is described in reference 2. A more recent, related procedure developed in the Langley Flutter Analysis Section has been employed in the present investigation.

The present paper is concerned with forces and moments associated with flapping oscillations of finite wings at low speeds. The plan forms treated are a rectangular wing of aspect ratio 2 and three tapered wings of aspect ratio 3 with varying amounts of sweepback. Initially, a correlation of theory and experiment for all four plan forms was intended and calculations for all four wings were made. Measurements, however, were actually made only for the rectangular wing; therefore, a comparison with theory is possible only for this case. Calculated aerodynamic forces for the other wings are also presented.

SYMBOLS

A aspect ratio

a distance from axis of rotation to wing-root fairing, positive for axis to left of root, ft (see sketch on page 7)

a_{nm} arbitrary coefficient in series expression for pressure distribution (see eq. (2))

b root semichord, ft

$C_{L,\phi}$, $C_{M,\phi}$, $C_{l,\phi}$ complex lift, pitching-moment, and rolling-moment coefficients; for example,

$$C_{L,\phi} = \left(C_{L,\phi}\right)_r + i\left(C_{L,\phi}\right)_i$$

$\left|C_{L,\phi}\right|$, $\left|C_{M,\phi}\right|$, $\left|C_{l,\phi}\right|$ magnitudes of complex lift, pitching-moment, and rolling-moment coefficients; for example,

$$\left|C_{L,\phi}\right| = \sqrt{\left[\left(C_{L,\phi}\right)_r\right]^2 + \left[\left(C_{L,\phi}\right)_i\right]^2}$$

$c_{l,\phi}$ section lift coefficient due to flapping oscillation

$f_n(\xi)$ chordwise pressure distribution function (see eq. (2))

$g_m(\eta)$ spanwise pressure distribution function (see eq. (2))

g_t damping coefficient of wing in airstream

g_{vac} damping coefficient of wing in near vacuum

h reference vertical displacement of wing tip, positive down, $h_o e^{i\omega t}$, ft

I_s effective moment of inertia of system about axis of rotation, lb-ft-sec^2

k reduced-frequency parameter, $b\omega/V$

K_s effective spring constant of oscillating system, ft-lb/radian

$K(M,k,x-\xi,y-\eta)$ kernel function of integral equation (see eq. (1))

L total lift, positive down, lb

$$L = \pi \frac{\rho V^2}{2} S \sum_j q_j C_{L,q_j}$$

l section lift, lb/ft

M Mach number

M_α total pitching moment, ft-lb

$$M_\alpha = \pi \frac{\rho V^2}{2} Sb \sum_j q_j C_{M,q_j}$$

M_ϕ total rolling moment, ft-lb

$$M_\phi = \pi \frac{\rho V^2}{2} Sb \sum_j q_j C_{\underline{l},q_j}$$

$\Delta p(\xi,\eta)$ pressure distribution, lb/sq ft

q_j angular generalized coordinate of jth degree of freedom (as used herein, q_j is replaced by ϕ to denote a flapping oscillation), $(q_j)_o e^{i\omega t}$, radians

S area of wing, sq ft

s wing semispan, ft

t	time, sec
V	stream velocity, ft/sec
$w(x,y)$	amplitude function of prescribed downwash (see eq. (5)), ft/sec
x,y,ξ,η	Cartesian coordinates
$z(x,y,t)$	vertical displacement of wing surface, positive down, $z(x,y)e^{i\omega t}$, ft
$\Lambda_{l/4}$, $\Lambda_{l/2}$	sweep angles of quarter-chord and midchord lines, respectively, deg
λ	taper ratio
ρ	density, slugs/cu ft
ϕ	generalized coordinate of angular displacement in flapping oscillation, $\phi_o e^{i\omega t}$, radians
$\varphi_{L,\phi}$, $\varphi_{M,\phi}$, $\varphi_{l,\phi}$	phase angles between lift, pitching moment, or rolling moment and displacement in flapping oscillation (positive phase angle indicates that lift or moment vector leads displacement), deg; for example, $\phi_{L,\phi} = \tan^{-1}\frac{(C_{L,\phi})_i}{(C_{L,\phi})_r}$
$\varphi_{l,\phi}$	phase angle associated with $c_{l,\phi}$, deg
ω	circular frequency of oscillation in airstream, radians/sec
ω_{vac}	circular frequency of oscillation in near vacuum, radians/sec

Subscripts:

i,r	imaginary and real components
o	maximum amplitude
2-dim	two-dimensional
3-dim	three-dimensional

SCOPE OF THE INVESTIGATION

The present investigation was undertaken with the aim of correlating analytically and experimentally determined aerodynamic forces on a series of wings undergoing flapping oscillations. Four plan forms are involved: a rectangular wing of aspect ratio 2 and three tapered wings of aspect ratio 3 with varying degrees of sweepback. The wings are shown in figure 1. The taper ratio of the swept wings is 0.5 and the midchord sweep angles are 0°, 25°, and 41.5°.

Experimental results have been obtained only for the rectangular wing. Tests were conducted in the Langley 2- by 4-foot flutter research tunnel. Mach numbers ranged from 0.09 to 0.41, Reynolds numbers from 0.65×10^6 to 2.85×10^6, and reduced-frequency parameters from 0.2 to 0.9. Calculated results are obtained for $M = 0$ for all four plan forms. Total lift, pitching moment, and moment about the flapping axis are presented. Some details of the analytical procedure are given in the next section.

ANALYTICAL INVESTIGATION

Aerodynamic force and moment coefficients for several finite wings undergoing flapping oscillations have been obtained analytically by use of a recently developed numerical solution of the following integral equation:

$$\frac{w(x,y)}{V} = \frac{1}{4\pi\rho V^2} \iint_S \Delta p(\xi,\eta)\, K(M,k,x-\xi,y-\eta)\, d\xi\, d\eta \qquad (1)$$

This equation relates a known distribution of downwash $w(x,y)$ to the unknown pressure distribution $\Delta p(\xi,\eta)$ acting on the wing surface S. The function $K(M,k,x-\xi,y-\eta)$ is the kernel of the integral equation and is discussed in detail in reference 3. The coordinate system related to the problem is shown in the following sketch:

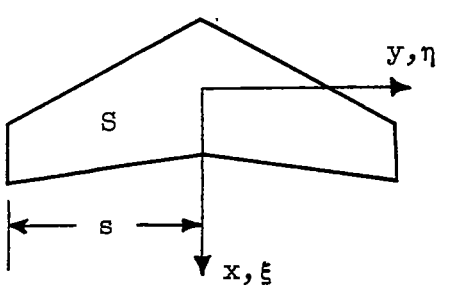

Solution of the Integral Equation

In the present study, equation (1) has been solved by the numerical procedure which has been recently developed in the Langley Flutter Analysis Section and programed for the IBM type 704 electronic data processing machine. The method used is related to that of reference 2, but involves a more exact expression for the kernel function and more refined methods of numerical integration.

As in the method of reference 2, it is assumed that the unknown pressure distribution in equation (1) can be represented by a series of chordwise and spanwise pressure modes containing arbitrary coefficients which must be determined. The series is of the form

$$\Delta p(\xi,\eta) = \sum_n \sum_m a_{nm} f_n(\xi) g_m(\eta) \tag{2}$$

where the functions $f_n(\xi)$ and $g_m(\eta)$ are the selected chordwise and spanwise pressure modes, respectively, and where a_{nm} represents the arbitrary coefficients.

Equation (2) is substituted into equation (1) to yield the following expression:

$$\frac{w(x,y)}{V} = \frac{1}{4\pi\rho V^2} \sum_n \sum_m a_{nm} \iint_S f_n(\xi) g_m(\eta) K(M,k,x-\xi,y-\eta) \, d\xi \, d\eta \tag{3}$$

The right side of equation (3) is simply a summation of definite integrals. Through this substitution the problem of solving the integral equation can be reduced to the solution of a system of algebraic equations, obtained by writing equation (3) for at least as many points (x,y) as there are unknown coefficients a_{nm} to be determined.

In the current procedure the integrals of equation (3) are evaluated by continuous numerical integration techniques, with special handling given to singularities in the pressure distribution and the kernel function. First, chordwise integrations are performed at many values of the spanwise variable η. Appropriate spanwise integration rules are then applied to complete the surface integration. This procedure is employed for each of several points (x,y), and appropriate values of the downwash function are applied at each point. A set of simultaneous equations is thus obtained which may be solved for the values of the coefficients a_{nm}. Substitution of these values into equation (2) provides an analytic expression for the continuous pressure distribution $\Delta p(\xi,\eta)$ associated

with the particular downwash distribution considered. This expression for the pressure distribution may then be used to obtain integrated quantities such as generalized aerodynamic forces required for flutter analysis, or section or total forces and moments. Before discussing these forces and moments, it is useful to consider first the type of wing motion and the form of the associated downwash distribution dealt with in the present study.

Wing Motion and Downwash Distribution

The wing motion treated in the present investigation is a symmetric flapping oscillation. The configuration dealt with analytically corresponds to that of the experimental tests. The wing is assumed to undergo rotation through an angle ϕ about an axis parallel to the airstream and located a distance a inboard of the wing root fairing. A mirror image of the portion of the wing exposed to the airstream is assumed to extend from the root fairing. The configuration is illustrated in the following sketch:

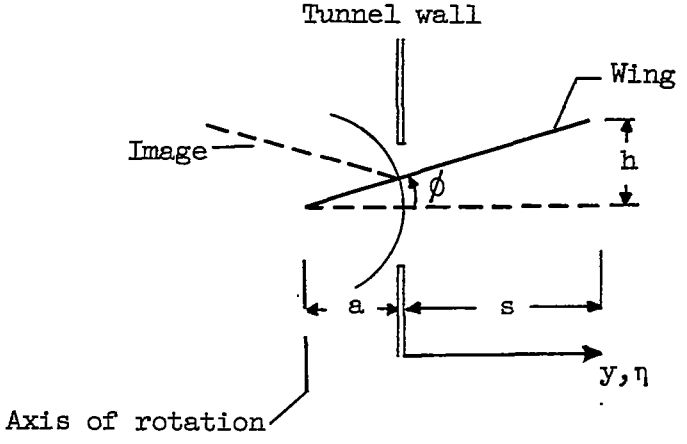

The vertical displacement $z(x,y,t)$ of the surface may be defined by the relation

$$z(x,y,t) = |y + a|\phi \tag{4}$$

where $\phi = \tan^{-1}\frac{h}{s + a}$. The downwash distribution $w(x,y)$ is then

given by

$$w(x,y) = -\left(V\frac{\partial}{\partial x} + i\omega\right)z(x,y) = -i\omega\left|y + a\right|\phi_o \tag{5}$$

or

$$\frac{w(x,y)}{V} = -ik\left|\frac{y + a}{b}\right|\phi_o \tag{6}$$

Equation (6) may be used together with equation (3) to obtain the values of the coefficients a_{nm} which define the pressure distribution $\Delta p(\xi,\eta)$.

Aerodynamic Force and Moment Coefficients

Certain integrated functions of the pressure distribution are of interest in the present study: total lift, total pitching-moment, and total rolling-moment coefficients. They are defined in the following manner:

Total lift -

$$\pi\frac{\rho V^2}{2}S\phi C_{L,\phi} = \iint_S \Delta p(\xi,\eta)\,d\xi\,d\eta \tag{7}$$

Total pitching moment (about axis $\xi = 0$) -

$$\pi\frac{\rho V^2}{2}Sb\phi C_{M,\phi} = \iint_S \xi\,\Delta p(\xi,\eta)\,d\xi\,d\eta \tag{8}$$

Total rolling moment (about axis of rotation) -

$$\pi\frac{\rho V^2}{2}Sb\phi C_{l,\phi} = \iint_S (\eta + a)\,\Delta p(\xi,\eta)\,d\xi\,d\eta \tag{9}$$

The quantities represented by equations (7), (8), and (9) have been evaluated for the rectangular wing dealt with in the experimental tests as well as for the three tapered wings.

Spanwise Variation of Lift Coefficient

The basic assumption of the strip-analysis method of flutter investigation is that each section is assumed to behave aerodynamically as though two-dimensional. The magnitude of the force acting on the section is given by the product of the two-dimensional coefficient appropriate to the motion of the section and the displacement of the section. For flapping motion, the section lift would be given by the product of the lift due to translation and the vertical displacement of the section; that is,

$$l = \pi\rho b^2\omega^2 L_h z(x,y)\phi$$

or

$$c_{l,\phi} = \frac{l}{\pi \frac{\rho V^2}{2} b\phi} = 2k^2 L_h \frac{z(x,y)}{b} \tag{10}$$

where $z(x,y)$ is the amplitude of the flapping mode and L_h is the two-dimensional lift coefficient due to translation.

In the presentation of results to follow, a section coefficient based on two-dimensional theory and defined by equation (10) is compared with the corresponding result from three-dimensional theory. The three-dimensional result is obtained from the chordwise integral of the pressure distribution as defined by equation (2); that is,

$$c_{l,\phi} = \frac{1}{\pi \frac{\rho V^2}{2} b\phi} \int_{\text{chord}} \Delta p(\xi,\eta)\, d\xi \tag{11}$$

EXPERIMENTAL INVESTIGATION

Apparatus

Tunnel.- The Langley 2- by 4-foot flutter research tunnel was used for the tests reported herein. All tests were made in air at a density of 1 atmosphere. The wing was mounted in the test section as shown in figure 2.

Wing model.- The semispan wing model had an exposed rectangular plan form with a 1-foot chord and a 1-foot span. The model was of thick-skin balsa construction covered with glass cloth and had an NACA 65A010 airfoil section. The wing was designed to have high natural frequencies

(relative to the forced frequency of oscillation which was approximately 30 cycles per second) in order to minimize elastic deformation and eliminate correction to the measured forces. The first natural cantilever bending frequency was 112 cycles per second and the first natural torsional frequency was 168 cycles per second.

The semispan wing model was mounted in an oscillating mechanism as shown in figure 2. This mechanism permitted the wing to oscillate in a flapping motion about an axis 0.5 foot inboard of the wing-root fairing through an angle of $\pm 3^{\circ}$. The wing model was dynamically balanced about this axis of oscillation by the use of a balance wing mounted out of the airstream in such a way that there were little lift and pitch reactions when the wing was oscillated in a near vacuum. A correction was made to the data to account for the apparent air mass on the balance wing.

Oscillating mechanism.- The oscillating mechanism is similar to the one described in reference 4. The oscillating mechanism may be considered as a simple torsional vibratory system as illustrated in figure 2. The system consists of a torsion spring or torque rod which is fixed at one end and a hollow steel trunnion which is supported by bearings mounted on force displacement dynamometers. Since the torque rod is parallel to the airstream, the wing oscillates in a flapping motion about the axis of the trunnion. A fairing was placed over, and moved with, the root of the wing model as indicated in figure 2. The mechanism was oscillated at the natural torsional frequency of the spring-inertia system by applying a harmonically varying torque through the shaker coil arms attached to the trunnion. This frequency of oscillation was 30 cycles per second with a flapping amplitude of $\pm 3^{\circ}$.

The electromagnetic shakers consisted of stationary coils furnishing a steady magnetic field and moving coils which were attached to the trunnion. The moving coils were alined so that the direction of the applied force was perpendicular to the direction of the lift; thus, any difference between the shaker forces would not be felt in the dynamometers.

Instrumentation and Calibration

The instrumentation provided signals that were a measure of the lift, lift phase angle, pitching moment, pitching-moment phase angle, and the components of the rolling moment. The lift and pitching moment and their associated phase angles were obtained from the output of the force-displacement dynamometers which converted the reactions on the trunnion bearing supports into electrical signals. These electrical signals were fed through amplifiers and filters to a vacuum-tube voltmeter to obtain the lift and pitching moment, and to a phasemeter to obtain the phase angles. The angular position ϕ was determined from a strain gage mounted on the torque rod. The dynamometer signals for pitching moment

were calibrated for moment referred to an axis passing through the root midchord line and perpendicular to the stream direction.

The signals from the dynamometers were calibrated in terms of pounds of force per unit of signal strength. The vacuum-tube voltmeter was calibrated dynamically by using a voltage divider referred to the open-circuit calibration of the strain gages. The vacuum-tube voltmeter readings are believed to be within ±4 percent of true signal.

All phase relationships were measured with an electronic phasemeter. The output from this phasemeter was read on an ammeter calibrated in degrees. This system was calibrated by using a standard resistance-capacitance phase-shift circuit with the results indicating that the phase angle may be determined within ±3° of true value.

The period of oscillation was determined with an electronic counter-chronograph by measuring the time lapse between corresponding points on the angular-position signal.

The angular-position signal from the strain gage was recorded on an oscillograph while the wing was oscillating at constant amplitude to obtain the amplitude of oscillation; the signal was also recorded during the decay of the oscillation to obtain the damping factor for the component of the rolling moment in phase with the angular velocity. A photographic technique was used to calibrate dynamically the angular position of the wing with the signal from the strain gage. Time exposures were taken of a fine spanwise line on the leading edge of the wing at various amplitudes while the signal output of the torsion strain gage was recorded. The amplitude of oscillation of the wing was obtained from the envelope of the line on the leading edge of the wing and correlated with the torsion-strain-gage signal.

Data Reduction

The magnitude of the lift and pitching moments was obtained directly by multiplying the output of the vacuum-tube voltmeter, recorded while the wing was oscillating at constant amplitude, by the appropriate calibration constant.

The component of the rolling-moment coefficient in phase with the angular velocity was determined from the logarithmic decrement of the power-off decay of the oscillation from the following relation:

$$\left(C_{\underline{l},\phi}\right)_i = -\frac{I_s\omega^2}{\pi\frac{\rho V^2}{2}Sb}\left[g_t - \left(\frac{\omega_{vac}}{\omega}\right)^2 g_{vac}\right] \qquad (12)$$

The derivation of equation (12) is shown in detail in appendix B of reference 4.

The component of the rolling-moment coefficient in phase with angular displacement was determined from a frequency shift from the resonant frequency of the oscillating system in a near vacuum. This component was determined from the equation

$$\left(C_{\underline{l},\phi}\right)_r = -\frac{K_s}{\pi \frac{\rho V^2}{2} Sb}\left[\left(\frac{\omega}{\omega_{vac}}\right)^2 - 1\right] \tag{13}$$

Additional information on obtaining this component is given in appendix A of reference 5.

RESULTS AND DISCUSSION

Lift and moment coefficients associated with flapping oscillations have been obtained for a rectangular wing by the analytical and experimental procedures described in preceding sections. In addition, analytical results have been obtained for three tapered plan forms having varying amounts of sweepback. Before discussing these results, the sign convention used should be described. The following definitions of positive displacement and positive force and moment vectors are employed:

(1) The vertical displacement of a point on the wing surface is considered to be positive down.

(2) The lift force is considered to be positive down.

(3) The pitching moment is chosen as positive when it tends to rotate the leading edge upward.

(4) The moment about the axis of rotation (in flapping) is considered positive when it tends to rotate the wing tip downward.

Results for Rectangular Wing

It is recalled that the rectangular wing under consideration is undergoing a flapping oscillation about an axis 0.5 foot inboard of the wing-root fairing. The surface of the wing exposed to the airstream has a 1-foot semispan and a 1-foot chord and, with its mirror image at the

tunnel wall, has an aspect ratio of 2. Calculations have been made at $M = 0$ and experimental data have been obtained for Mach numbers between 0.1 and 0.4. Theoretical and experimental values of total lift and moment coefficients are presented in table I and figure 3; section lift coefficients obtained from two- and three-dimensional theory are shown in figure 4.

Comparison of theoretical and experimental results for total lift and moment coefficients.- The theoretical and experimental values of total lift and moment coefficients and the associated phase angles are shown plotted against reduced-frequency parameter k in figure 3. Figure 3(a) indicates that although the trends are similar, the experimentally and theoretically determined lift coefficients and the associated phase angles differ by nearly constant amounts as k is varied. The theoretical and experimental results for the pitching-moment coefficient shown in figure 3(b) are in excellent agreement; the associated phase angles, however, indicate different trends, the variation of k having less effect on the theoretical values than on the experimental values. The results for the rolling moment are given in figure 3(c). Again, the magnitudes of the moment are in fairly good agreement; the phase angles exhibit similar trends but differ considerably in value, particularly as the reduced-frequency parameter is increased. The calculated values of the phase angles associated with rolling moment are very near the calculated values of the phase angles associated with lift shown in figure 3(a).

Comparison of results of two- and three-dimensional theory for section lift coefficient.- For the purposes of making a flutter analysis, a knowledge of section coefficients rather than total coefficients is required. As a matter of interest, results of two- and three-dimensional theory for section lift coefficient and associated phase angles are shown in figure 4 for three values of reduced-frequency parameter k. Since the mode of displacement under consideration varies linearly with y, the section lift coefficient based on two-dimensional theory (see eq. (10)) also varies linearly with y. The section coefficient based on three-dimensional theory (see eq. (11)), on the other hand, reduces to zero at the wing tip. The area under the curves representing the three-dimensional section lift coefficients corresponds to the total lift coefficients plotted in figure 3(a). These are repeated and compared with results obtained from the two-dimensional values in the following table:

k	$\lvert C_{L,\phi} \rvert_{3\text{-dim}}$	$\lvert C_{L,\phi} \rvert_{2\text{-dim}}$
0.22	0.312	0.631
.6	.976	1.443
.8	1.453	1.992

Results for Tapered Wings

Calculated results for the lift and moments on the three tapered wings illustrated in figure 1 are given in figure 5. Figure 5(a) shows the lift coefficients and the associated phase angles for the three wings. As k is increased, the lift coefficients increase and the phase angles all become less negative. The pitching moment (fig. 5(b)) and rolling moment (fig. 5(c)) and the associated phase angles follow trends similar to those indicated for the lift as k is increased. The greatest effect of change in plan form occurs in the pitching moment. The pitching moment shown in figure 5(b) is referred to an axis passing through the root midchord line and perpendicular to the stream direction. The change in pitching moment for the various plan forms indicates a shift in location of center of pressure relative to this axis.

CONCLUDING REMARKS

Lift and moment coefficients associated with flapping oscillations have been obtained for a rectangular wing by an analytical and an experimental procedure. In addition, analytical results have been obtained for three tapered plan forms having varying amounts of sweepback. In general, for the rectangular wing, the lift coefficients and the associated phase angles obtained from theory and experiment show the same trends over the reduced-frequency range investigated but differ by nearly constant amounts. The values of the theoretical and experimental pitching-moment coefficients are in excellent agreement; the associated phase angles, however, show different trends. The theoretical and experimental values of the rolling-moment coefficients are also in fairly good agreement, but the phase angles differ considerably in value. Calculated values of phase angles associated with rolling moment are quite near those associated with lift. The calculated values of total forces and moments based on lifting-surface theory included for the three tapered wings show that the greatest effect of change in plan form occurs in the pitching moment; lift and rolling moment are much less affected.

Langley Aeronautical Laboratory,
National Advisory Committee for Aeronautics,
Langley Field, Va., May 23, 1958.

REFERENCES

1. Widmayer, Edward, Jr., Clevenson, Sherman A., and Leadbetter, Sumner A.: Some Measurements of Aerodynamic Forces and Moments at Subsonic Speeds on a Rectangular Wing of Aspect Ratio 2 Oscillating About the Midchord. NACA TN 4240, 1958. (Supersedes NACA RM L53F19.)

2. Runyan, Harry L., and Woolston, Donald S.: Method for Calculating the Aerodynamic Loading on an Oscillating Finite Wing in Subsonic and Sonic Flow. NACA Rep. 1322, 1957. (Supersedes NACA TN 3694.)

3. Watkins, Charles E., Runyan, Harry L., and Woolston, Donald S.: On the Kernel Function of the Integral Equation Relating the Lift and Downwash Distributions of Oscillating Finite Wings in Subsonic Flow. NACA Rep. 1234, 1955. (Supersedes NACA TN 3131.)

4. Clevenson, Sherman A., and Leadbetter, Sumner A.: Some Measurements of Aerodynamic Forces and Moments at Subsonic Speeds on a Wing-Tank Configuration Oscillating in Pitch About the Wing Midchord. NACA TN 3822, 1956.

5. Clevenson, Sherman A., and Widmayer, Edward, Jr.: Experimental Measurements of Forces and Moments on a Two-Dimensional Oscillating Wing at Subsonic Speeds. NACA TN 3686, 1956. (Supersedes NACA RM I9K28a.)

TABLE I

ANALYTICAL AND EXPERIMENTAL VALUES OF COEFFICIENTS FOR A RECTANGULAR WING UNDERGOING A FLAPPING OSCILLATION

[A = 2; M = 0]

k	$\lvert C_{L,\phi}\rvert$	$\varphi_{L,\phi}$, deg	$\lvert C_{M,\phi}\rvert$	$\varphi_{M,\phi}$, deg	$\lvert C_{\underline{l},\phi}\rvert$	$\varphi_{\underline{l},\phi}$, deg
Analytical						
0.22	0.312	-77.8	0.192	86.6	0.600	-77.5
.6	.976	-57.5	.493	84.3	1.886	-56.8
.8	1.453	-49.7	.639	83.6	2.822	-49.1
Experimental						
0.203	0.354	-65	0.2028	99	0.48	-83
.208	.366	-64	.2133	99	.48	-83
.214	.369	-63	.2142	98	.48	-82
.218	.369	-64	.2100	97	.48	-82
.227	.384	-62	.2172	96	.51	-82
.234	.402	-62	.2295	96	.51	-81
.240	.405	-62	.2286	95	.51	-81
.252	.432	-59	.2394	96	.54	-81
.254	.441	-58	.2445	94	.60	-81
.275	.465	-57	.2598	94	.63	-81
.288	.471	-58	.2601	94	.63	-80
.307	.495	-56	.2898	93	.69	-79
.333	.537	-56	.2898	90	.78	-79
.358	.609	-60	.3132	90	.84	-78
.378	.639	-58	.3216	81	.93	-78
.433	.771	-56	.3714	84	1.05	-76
.492	.876	-49	.4023	76	1.29	-75
.542	.960	-46	.4455	79	1.59	-75
.649	1.203	-37	.5094	79	1.68	-70
.719	1.368	-39	.5388	67	2.01	-70
.910	1.935	-30	.6777	72	2.71	-66

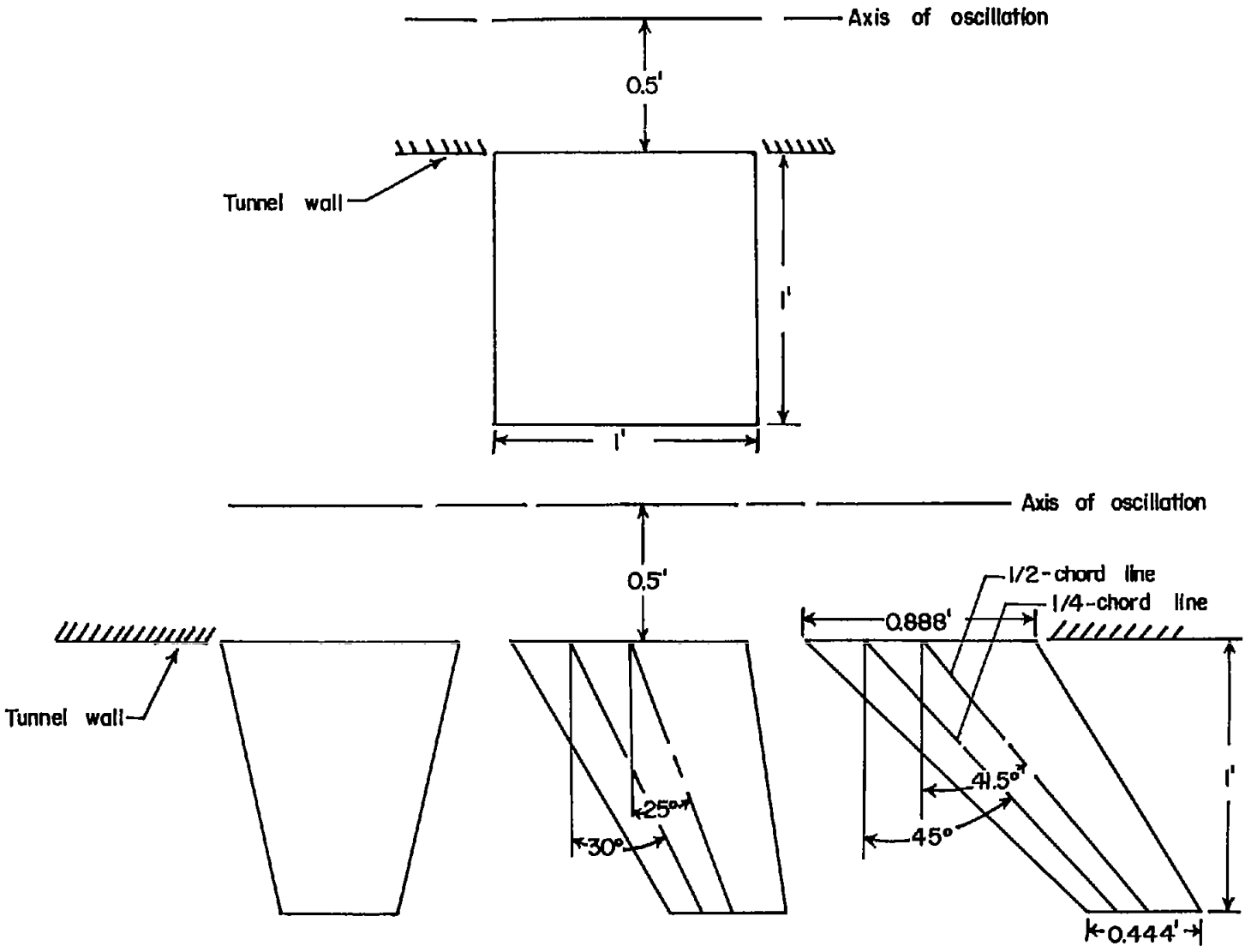

Figure 1.- Plan forms considered in investigation.

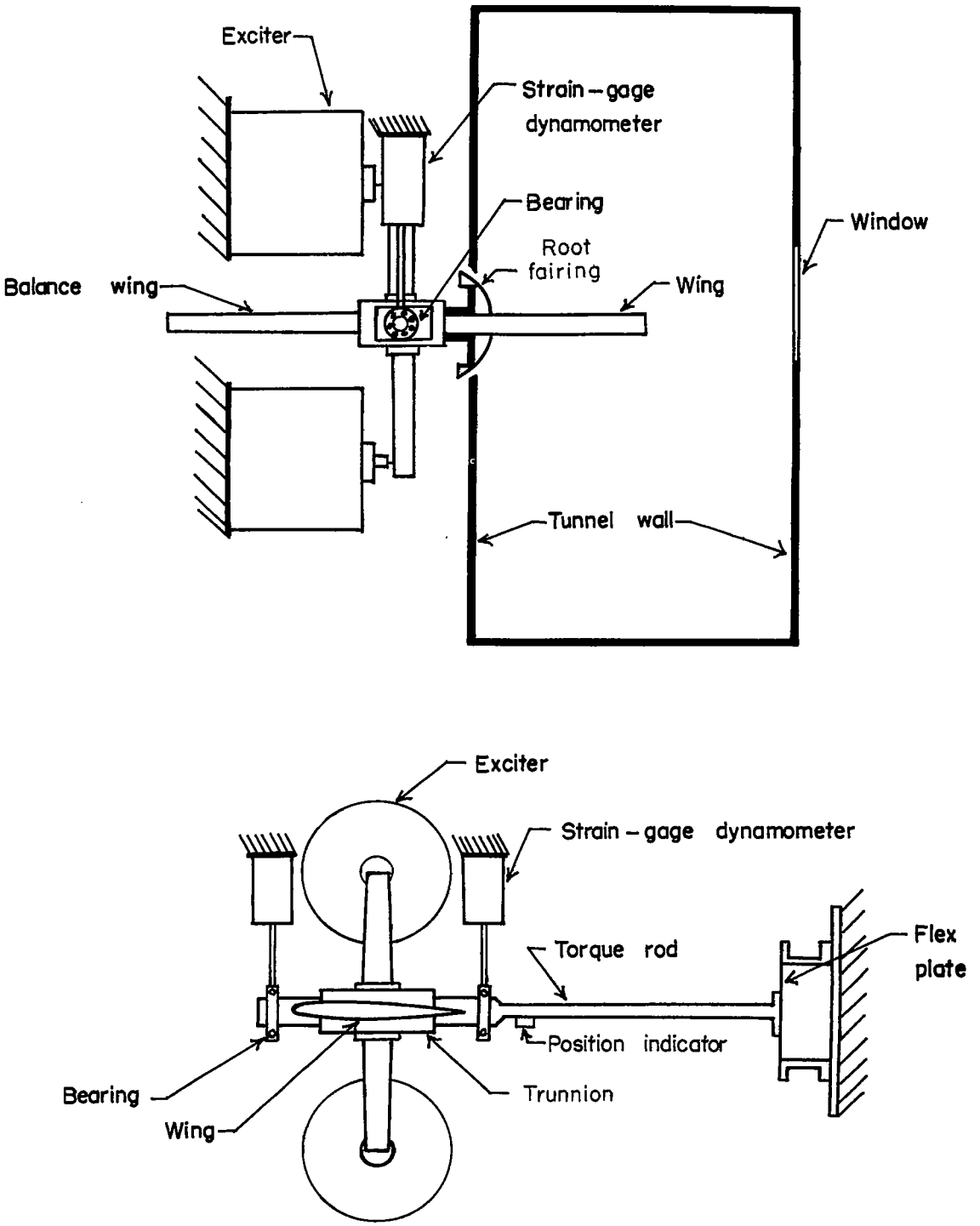

Figure 2.- Diagrammatic view of wing and oscillating mechanisms in the Langley 2- by 4-foot flutter research tunnel.

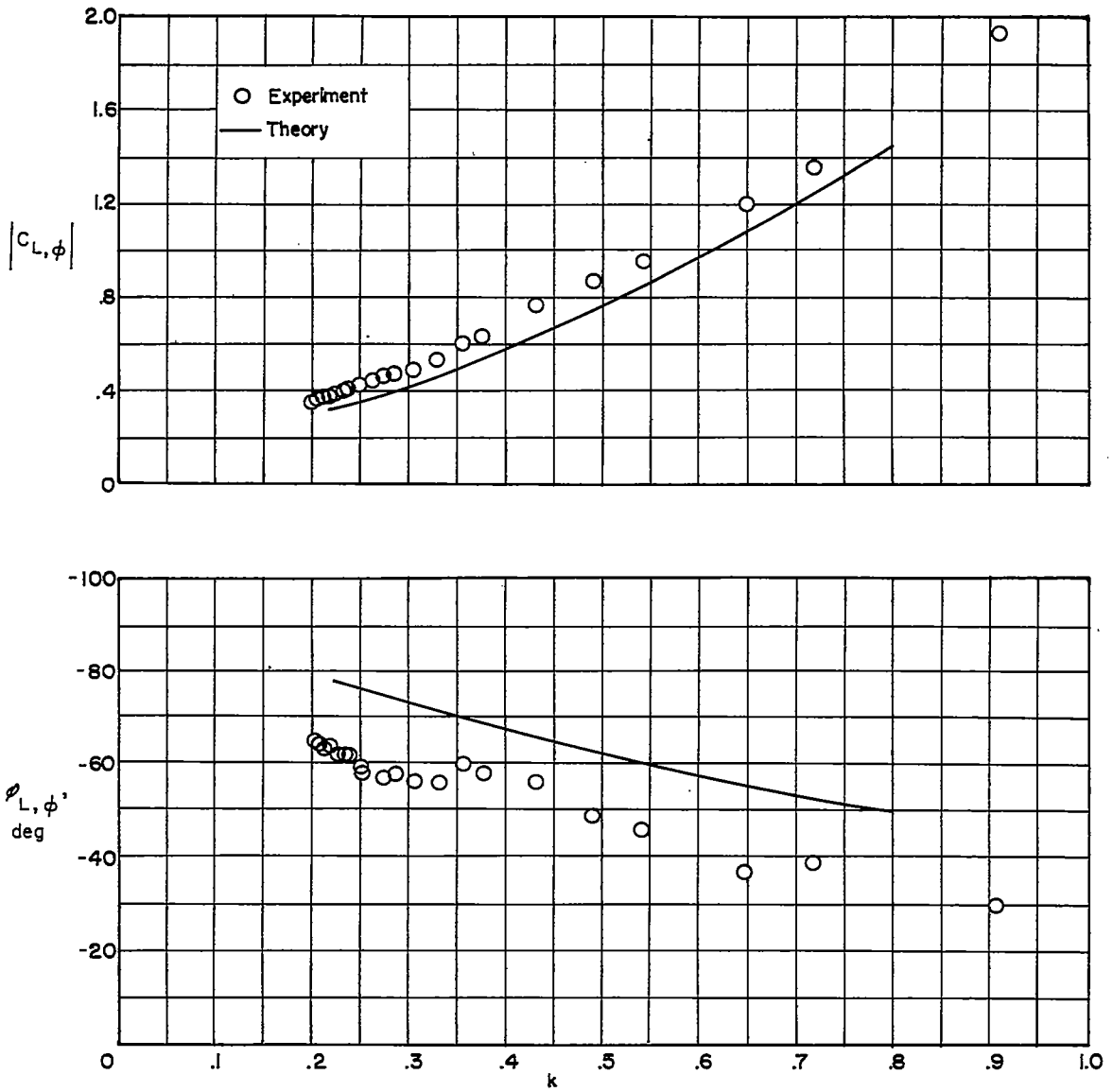

(a) Lift.

Figure 3.- Comparison of theoretical and experimental lift and moment coefficients and associated phase angles plotted against reduced-frequency parameter for rectangular wing undergoing flapping oscillations. M = 0; A = 2.

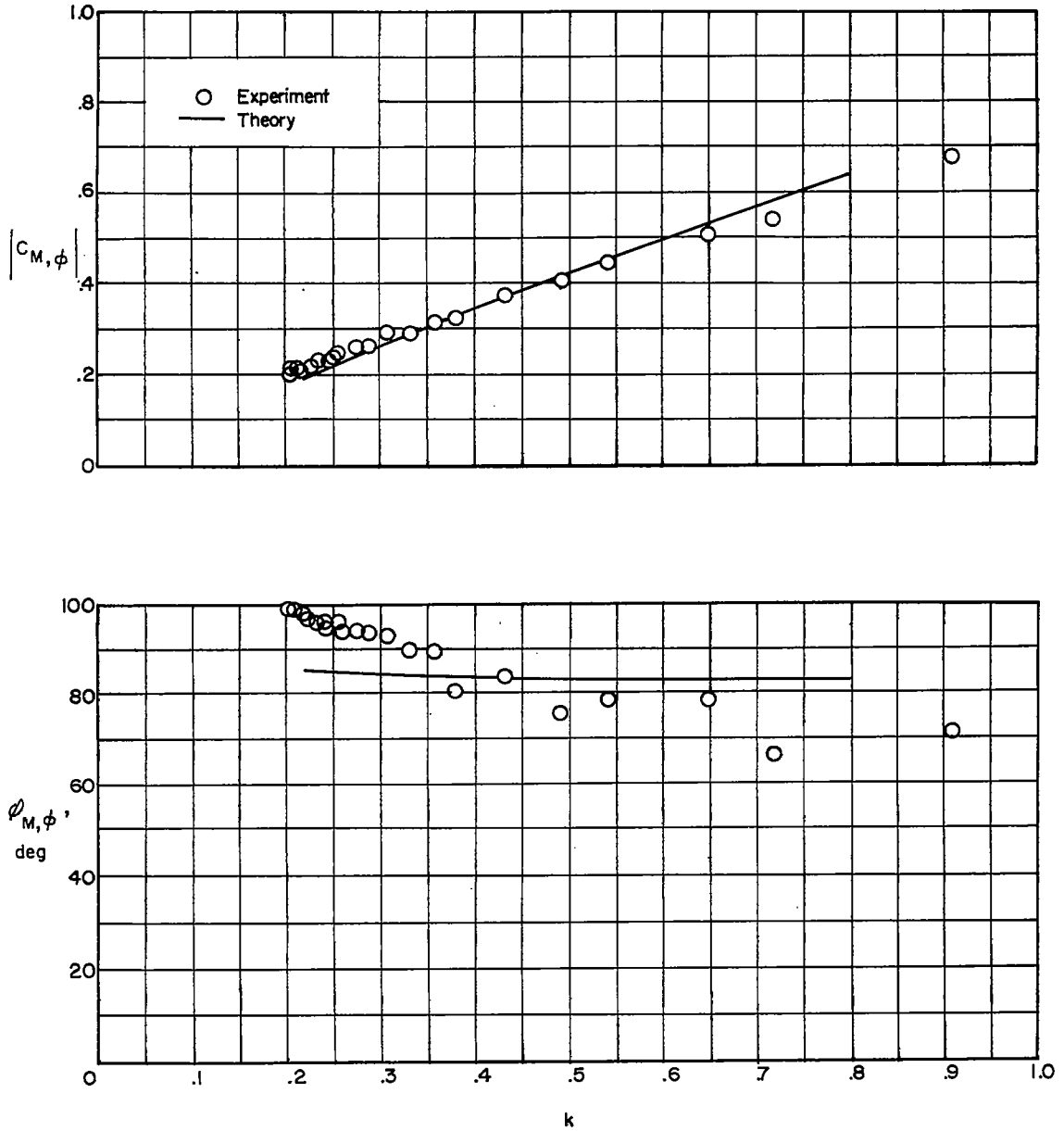

(b) Pitching moment about $\xi = 0$.

Figure 3.- Continued.

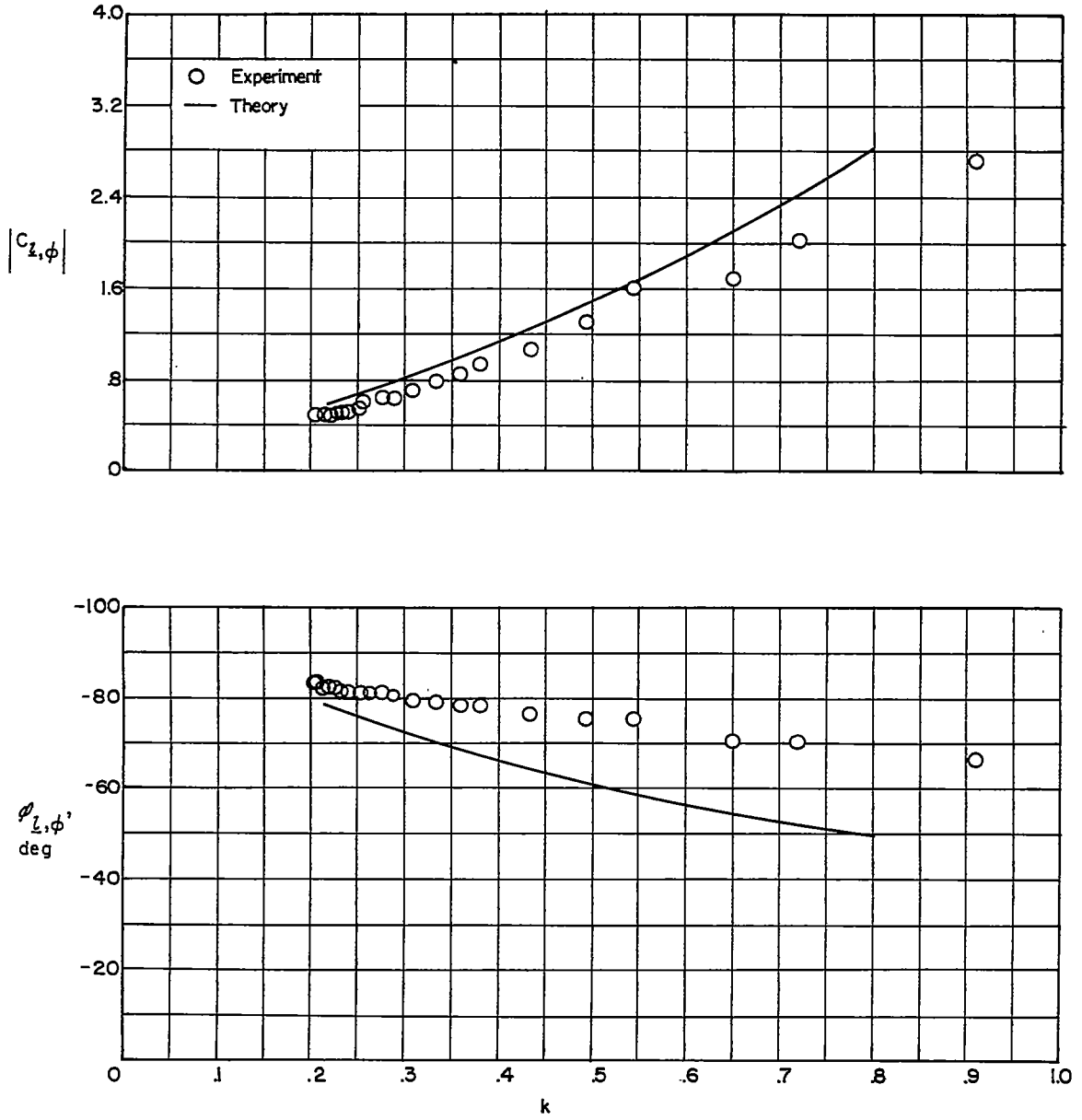

(c) Rolling moment about axis of rotation.

Figure 3.- Concluded.

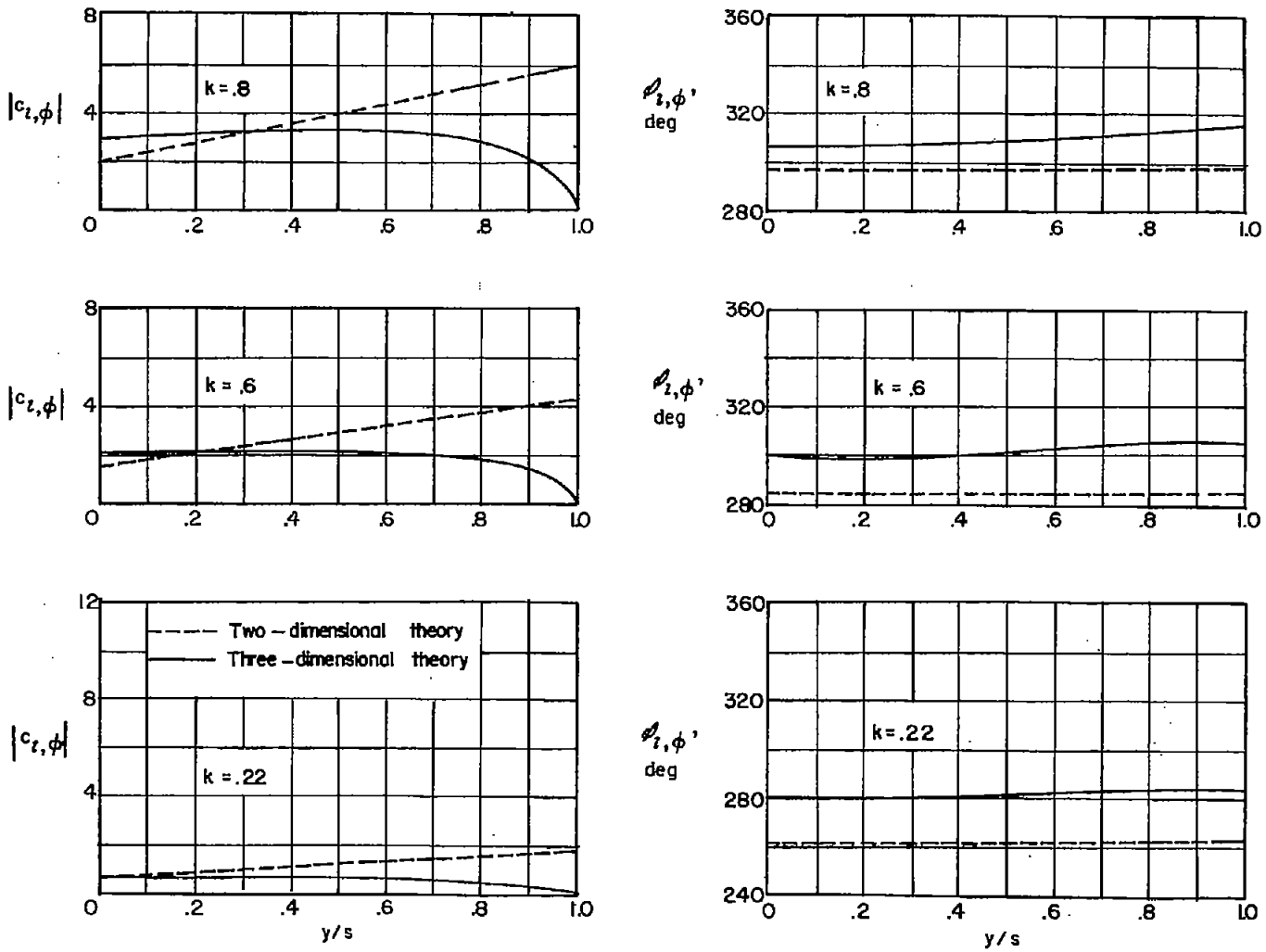

Figure 4.- Comparison of results of two- and three-dimensional theory for section lift coefficients and associated phase angles for rectangular wing undergoing flapping oscillations. M = 0; A = 2.

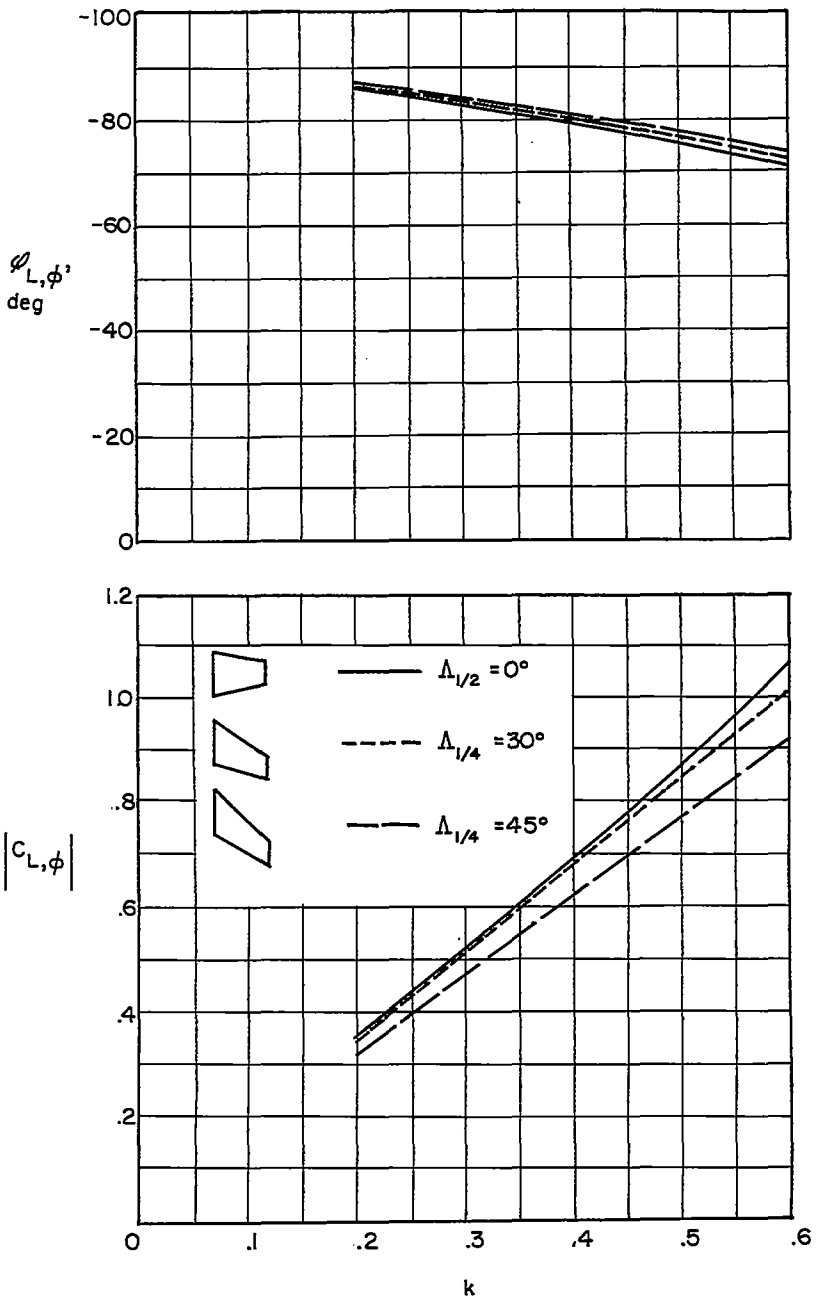

(a) Lift.

Figure 5.- Variation of lift and moment coefficients and associated phase angles with reduced-frequency parameter for three tapered wings undergoing flapping oscillations. (Results calculated at M = 0.)

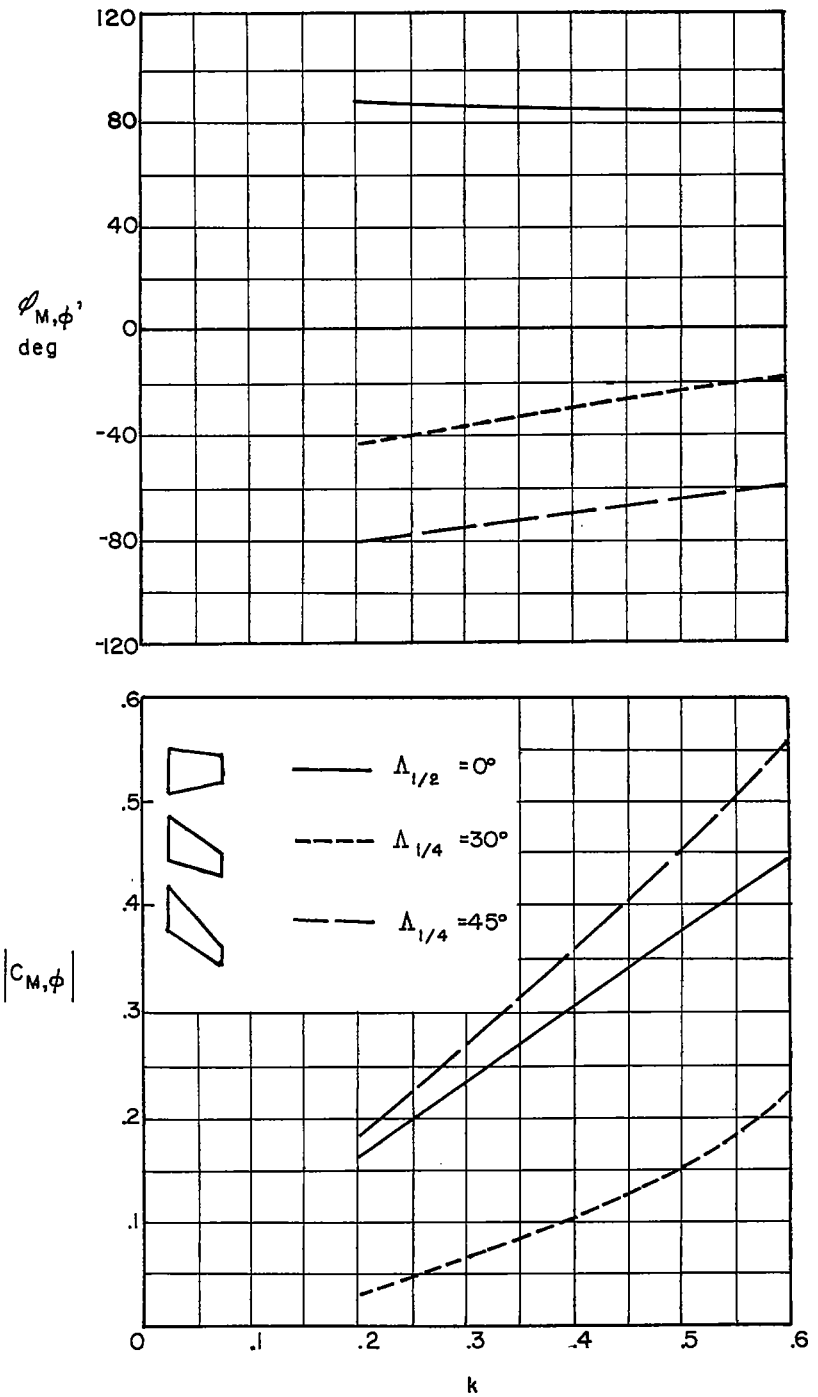

(b) Pitching moment about $\xi = 0$.

Figure 5.- Continued.

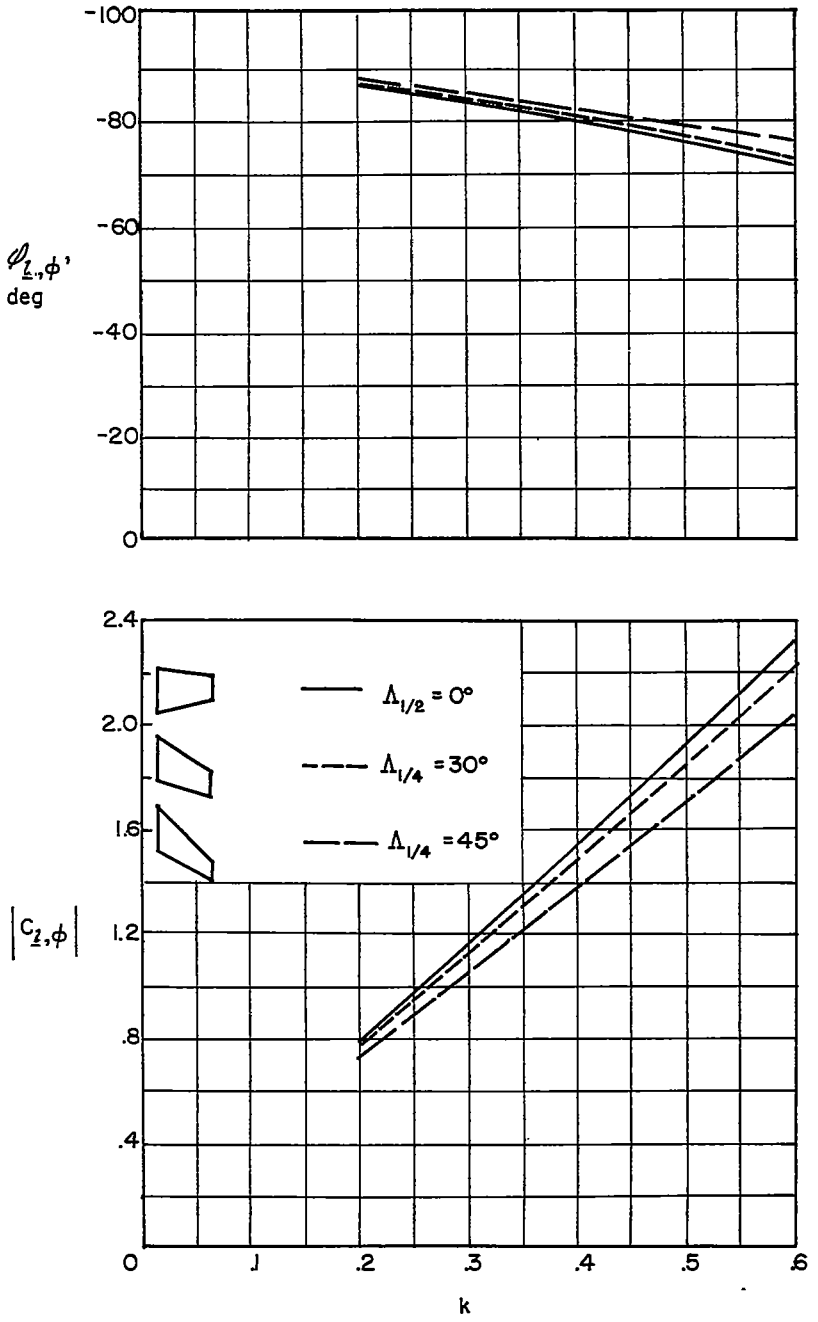

(c) Rolling moment about axis of rotation.

Figure 5.- Concluded.

NACA - Langley Field, Va.